Correction of Data Gathered by Degraded Transducers for Damage Prognosis in Composite Structures

K. R. Mulligan[1], N. Quaegebeur[2], P. Masson[3], and S. Létourneau[4]

[1,2,3] *Université de Sherbrooke, Sherbrooke, QC, J1K 2R1, CANADA*
Kyle.Mulligan@USherbrooke.ca
Nicolas.Quaegebeur@USherbrooke.ca
Patrice.Masson@USherbrooke.ca

[4] *NRC–IIT, National Research Council of Canada, Ottawa, ON, K1A 0R6, CANADA*
Sylvain.Letourneau@nrc–cnrc.gc.ca

ABSTRACT

This paper presents an approach for the correction of data gathered for damage prognosis (DP) in composite structures. The validation setup consists of surface-bonded piezoceramic (PZT) transducers used in a Structural Health Monitoring (SHM) system with simulated bonding layer damage using Teflon masks. The modal damping around PZT mechanical resonance is used as a metric to assess and compensate for the degradation of the adhesive layer of the transducers. Modal damping is derived from electrical admittance curves using a lumped parameter model to monitor the degradation of the transducer adhesive layer. A Pitch-Catch (PC) configuration is then used to discriminate the effect of bonding degradation on actuation and sensing. It is shown that below the first mechanical resonance frequency of the PZT, degradation leads to a decrease in the amplitude of the transmitted and measured signals. Above resonance, in addition to a decrease in signal amplitude of the transmitted and measured signals, a slight linear phase delay is also observed. A Signal Correction Factor (SCF) is proposed to adjust signals based on adhesive degradation evaluated using the measured modal damping. The benefits of the SCF for prognostics feature generation are demonstrated in the frequency domain for the A_0 mode.

1. INTRODUCTION

Structural Health Monitoring (SHM) denotes in-situ and continuous on-line monitoring (Mickens, Schulz, Sundaresan, & Ghoshal, 2003) for detection and interpretation of adverse changes within a structure (Kessler & Pramila, 2007). SHM is applicable to a number of fields aiming at reducing system life-cycle costs and down-time and increasing safety (Giurgiutiu & Bao, 2004). In the aerospace domain, this is done by integrating Non-Destructive Evaluation (NDE) techniques as autonomous systems into airframes (Kessler & Pramila, 2007). Increasing confidence in SHM solutions could also contribute to reduce maintenance costs by minimizing scheduled downtime through decreasing the frequency and duration of these maintenance intervals (Kapoor, Boller, Giljohann, & Braun, 2010). Such failures depend on the host structure material which is typically aluminum or a Carbon Fiber Re-inforced Polymer (CFRP).

Data gathered from SHM systems for airframe diagnostics are used to detect and localize fatigue damage only. SHM systems based on Guided Wave (GW) propagation using piezoceramic transducers are among the various existing systems that could be used for data gathering. Piezoceramic transducers are advantageous due to their cost-effectiveness and lightweight and can be used for quick and continuous structural inspections (Quaegebeur, Masson, Langlois-Demers, & Micheau, 2010).

Prognostic enhancements are currently being investigated for SHM systems to improve condition-based monitoring. Damage prognosis (DP) is defined as an estimate of an engineered system's Remaining Useful Life (RUL) (Farrar & Lieven, 2007). These enhancements aim to monitor tendencies within SHM data to classify the various airframe failure modes (Kessler & Pramila, 2007) and then estimate the RUL of the host structure.

The use of CFRPs for host structure fabrication has increased as reported by (Kessler & Pramila, 2007). For CFRPs, the two main failure modes due to impacts include intra-ply matrix cracking and inter-ply delaminations. Intra-ply matrix

cracking occurs on the host structure surface due to low impact energies prior to inter-ply delaminations. Inter-ply delaminations are the result of either singular high energy impacts or repeated low velocity impacts which also cause intra-ply matrix cracks to spread and weaken the host structure as described in (Iarve, Gurvich, Mollenhauer, Rose, & Dávila, 2011). Prediction using model-based prognostics of inter-ply delamination size versus increasing impact projectile velocity is reported in (Mueller et al., 2009) where a numerical model is used to simulate an impact using a steel ball projectile (Choi, 1990). Their work did not follow ASTM standards that dictate a 16 mm hemispherical impact head must be used to impact composite coupons with a mass and height based on the coupon thickness such that realistic and repeatable damages (over a number of coupons) are induced (ASTM, 2007). Preliminary work described in (Ahmad & Gupta, 2010) for simulating and predicting the failure behavior of composite panels follows the ASTM standard for damage initiation but also presents only numerical results. Further numerical work for predicting crack growth and RUL are presented in (Coppe, Pais, Kim, & Haftka, 2010). In this work, crack growth RUL estimation is predicted using material properties and the stress intensity factor which is a complicated function of applied loading, boundary conditions, crack location, geometry, and material properties.

In the aforementioned numerical work, features are extracted from the simulations to form a feature set. The most representative and discriminate features from the set are then used as inputs to predictive models such as: K-Nearest Neighbor (KNN), Neural Networks, and Decision Trees. For GW, discriminative features are extracted from time, frequency, and energy domain signals (Kessler & Pramila, 2007). There is little knowledge however on which features can predict gradual tendencies from damage initiation which is important for RUL estimation and at what point these features can be used for RUL prediction after the damage initiation phase commences. Although much numerical work is presented in literature for damage prognosis and generating feature sets, there is little numerical work and nearly no experimental work in RUL estimation. Experimentally, little work has been put forth in proposing a robust data gathering methodology in a laboratory environment. Most successful RUL estimation approaches in various domains use a hybrid system that implements a combination of model and data driven based prognostics (Byington, Roemer, & Gallie, 2002).

An important consideration when using a piezoceramic transducer SHM system for data gathering prior to prognostic model development, is that impacts inflicted upon aerospace structures causes both structural damage and damage to the SHM system. More specifically, it is shown in (Park, Farrar, Lanza di Scalea, & Coccia, 2006) that impacts in regions around piezoceramic SHM systems mainly damage the bonding layer between the transducers and the host structure surface. Degradation of the bonding layer in turn affects the signals generated and received by these transducers shown in (Mulligan, Quaegebeur, Ostiguy, Masson, & Létourneau, 2012) for a glass plate as the host structure. Numerical simulations were used to determine a damage metric based on modal damping of the transducer determined from electrical admittance curves to assess the level of bonding layer degradation. A Signal Correction Factor (SCF) has been proposed to correct for changes in signal amplitude and phase caused by degradation which is measured from changes in modal damping. Numerical results of the modal damping metrics capability of measuring the amount of bonding layer degradation are verified experimentally due to the transparency of the glass host structure as chemical degradation was used.

In this paper, the modal damping metric is used to assess the amount of bonding layer degradation on a CFRP host structure numerically. Experimental measurements are used to validate numerical results by controlling the bonding coverage area of piezoceramic lead-zirconate-titanate (PZT) transducers using Teflon masks. Following this, two transducers are bonded to an aerospace grade CFRP plate in a Pitch-Catch (PC) configuration. One transducer is perfectly bonded to the structure as a reference whereas the other is bonded using Teflon masks in order to simulate a damage in the adhesive. Following the Pitch-Catch measurements, the damaged transducer is removed, the surface of the plate is cleaned, and a new transducer is bonded using a different Teflon mask. The Pitch-Catch measurements are repeated. During acquisition, the reference and damaged transducer take turns as an actuator or sensor and data are post processed to investigate the effect of degradation on actuation and sensing. A SCF is proposed to adjust the amplitude and phase of the measured signals based on bonding layer degradation using the modal damping metric. The SCF is used to adjust the A_0 dispersion curve to account for bonding layer degradation to demonstrate its importance in ensuring a robust database is gathered for later prognostic model development.

2. BONDING LAYER DEGRADATION MODES DUE TO IMPACTS

The effect of structural damage due to impacts on the bonding layer between a PZT transducer and the host structure has not been explicitly studied. Much work has however been done on the effect of impacts on adhesive bonded joints. The adhesive layer in composite lap joints with traction and impact loading remains intact while failure occurs at the adherends. Further damage propagation in the adherends causes the adhesive to gradually debond at the extremities of the lap joint (Galliot, Rousseau, & Verchery, 2012). Although a major portion of the impact energy is absorbed by the adherends, the remaining energy is transferred to the adhesive layer itself. With increasing impact energies, the adhesive layer is susceptible to failure modes including: a reduction in initial

Item	Material	Thickness (mm)	Young's Modulus (GPa)	Poisson's ratio	Density (kg/m^3)
PZT	PZT 5A	0.5	65.0	0.31	7750
CFRP	16 plies prepreg [0,90]8s	2.45	74.5	0.219	1488
Adhesive	Permatex® cyanoacrylate	0.1	2.4	0.3	1100

Table 1. Properties of the PZT transducer, CFRP, and adhesive layer.

contact areas through particle deformation and delamination due to shearing motion (Islam & Chan, 2004). The remaining impact energy does not however affect the Young's modulus for brittle adhesives (such as cyanoacrylate) (Sugaya, Obuchi, & Chiaki, 2011). The lack of resistance to impact damage of adhesives is primarily related to their density. Although density does not change with increasing impact energy, there is a lesser effect of damage on the adhesive layer if it has a high density core due to reduced buckling (Nguyen, Jacombs, Thomson, Hachenberg, & Scott, 2005).

3. Piezoceramic debonding metrics

For SHM system health verification, variations in the electrical admittance have been shown to play a meaningful role in the detection of transducer debonding from host structure surfaces under environmental and mechanical loading conditions (Park et al., 2006) (Mulligan et al., 2012). The electrical admittance of a piezoceramic transducer $\gamma(\omega)$ is defined as the ratio between the resulting current I and voltage V at a given angular frequency ω. The theoretical admittance is approximated using a lumped parameter system using a simple RC series model when neglecting the mechanical resonance of the PZT transducer. This model is shown (Mulligan et al., 2012) to provide a good approximation of the low frequency admittance but performs poorly for higher frequencies due to the occurrence of resonances which cannot be modeled. Therefore, around and above resonance, a basic LCR circuit shown in Fig. 1 must be used with series resistance R_s, electrostatic capacitance C_s, electrical compliance C_p, mechanical mass L_p, and mechanical damping R_p, where R_s and R_p account for energy dissipation (Kim, Grisso, Kim, Ha, & Inman, 2008).

$$\xi = \frac{1}{2R_\mathrm{p}}\sqrt{\frac{L_\mathrm{p}}{C_\mathrm{p}}} \tag{1}$$

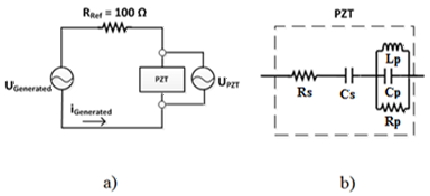

Figure 1. Admittance measurement circuit (a). RLC model of an unloaded PZT that accounts for mechanical resonance and damping (b).

From the electrical admittance curves, the modal damping ξ described by Eq. (1), which has been shown to describe gradual transducer debonding on a glass host structure, is extracted from estimation of the lumped parameter system (Mulligan et al., 2012). The constants of the lumped parameter system are determined by minimizing the distance between modeled and measured admittances for both the real and imaginary parts. Minimization algorithms are used to find the minimum of constrained multi-variable functions by substituting values for all variables using an initial estimate over a number of iterations and are available within the MATLAB framework (*fmincon* & *ga*).

The modal damping metric can be used to assess the level of adhesive coverage degradation and using the amplitude and phase change curves constructed for a particular host structure, a Signal Corrector Factor (SCF) can be developed as described in the next section.

4. Experimental and Numerical quantification of piezoceramic bonding layer degradation

4.1. Numerical assessment of the degradation process

The first step in this study is to investigate the degradation process of bonded PZTs and relate it to the modal damping metric extracted from the electro-mechanical problem in section 3. To do this, a numerical model has been developed (shown in Fig. 2) using commercial FEM software COMSOL. An axisymmetric 2D model in the frequency domain has been used for simplicity and to reduce computation time. To mimic the experimental setup presented later in section 4.2, a 5 mm circular PZT is attached to a 2.5 mm quasi-isotropic carbon fiber plate using a 0.1 mm thick bonding layer whose properties (shown in Tab. 1) are representative of cyanoacrylate. The carbon fiber plate is modeled as an isotropic structure using equivalent properties (shown in Tab. 1) obtained from mechanical testing of the orthotropic plate used experimentally and Perfectly Matched Layers (PML) of 20 mm are used to avoid boundary reflections.

The model is meshed using 15 000 triangular elements for a total number of 60 000 degrees of freedom (DOF) such that a maximum mesh size of 0.1 mm is ensured and that at least 10 nodes exist per minimum resolvable wavelength. A voltage of 1V is simulated at the upper electrode of the PZT and current is estimated at the same electrode to extract the electrical admittance. The modal damping ξ is estimated using methods described in section 3. In this numerical work, the variation of adhesive coverage degradation mode is tested. The

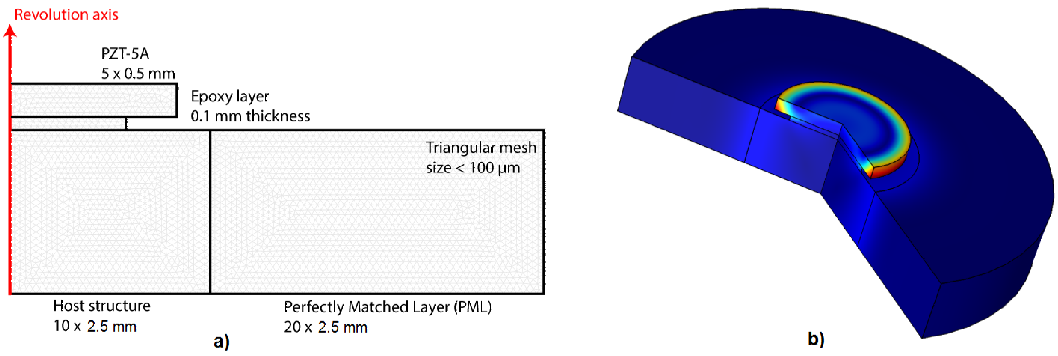

Figure 2. Illustration of the FEM mesh used for computation (a) and 3D reconstruction of the displacement field (b).

influence of adhesive coverage is estimated by changing the adhesive surface from 100 % (perfectly bonded adhesive) to 25 % (nearly debonded) by steps of 10 %. The results of the simulation are presented together with experimental results in section 4.3.

4.2. Experimental procedure

Experiments are carried out to relate the degradation process for bonded PZTs to the modal damping metric extracted from the electro-mechanical problem through gradual degradation. Transducers are bonded to the surface of a carbon fiber plate with dimensions 52 cm x 52 cm using 0.01 ml of cyanoacrylate measured from a syringe and a static load of 125 kPa. Adhesive coverage reduction was controlled using Teflon inserts during the PZT bonding process as in (Lanzara, Yoon, Kim, & Chang, 2009). Teflon is ideal for controlling the adhesive coverage under the PZT due to its low modulus of elasticity (Dupont, 2012). Almost no energy is transferred through the Teflon from the PZT into the structure leaving the remaining bonding layer as the conductive path. Adhesive coverage reduction using Teflon is chosen in this work as the primary adhesive failure mode because adhesive coverage is easily controlled experimentally compared to changes in the bonding layer Young's modulus which is degraded using ultraviolet (UV) light or temperature cycling and measured using traction testing or a rheometer which both require access to the adhesive under the PZT (Lotters, Olthuis, Veltink, & Bergveld, 1997). The Young's modulus effect is considered as negligible (Skaja, Fernando, & Croll, 2006).

Voltage bursts are generated at the PZT, and the impedance is measured using a voltage divider circuit with a 100 Ω 5 % resistor. The input signals are generated using an HP33120A generator with a sampling frequency of 10 MHz. The generated signals are amplified using a MusiLab UA-8400 amplification system. The signal acquisition is performed using a high impedance National Instruments® PCI-5105 12-bit DAQ board configured through a custom LabVIEW interface. The signals are recorded at a fixed sampling frequency of 10 MHz. All measurements are averaged 500 times in order to increase SNR and low-pass filtered at 1.5 MHz. The transfer function for the admittance over the entire frequency range below 1 MHz is obtained using broadband generation of guided waves through sub-band decomposition with N = 11 sub-bands for reconstruction between 10 kHz and 1 MHz as presented in (Quaegebeur, Masson, Micheau, & Mrad, 2012). A sub-band frequency step of 100 kHz is selected to ensure perfect reconstruction. The modal damping is extracted from the admittance curve as described in (Mulligan et al., 2012).

4.3. Numerical and experimental results of bonding layer degradation

The numerical and experimental results for modal damping for 4 degradation trials and the unbonded case are presented in Fig. 3. Simulations show that modal damping decreases with degradation over a range of 85 %. Experimentally, the same

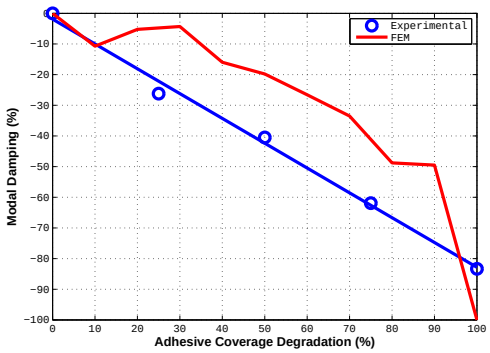

Figure 3. Numerical and experimental results for modal damping over adhesive coverage degradation.

tendencies are observed as in the simulated curve with good agreement. For a linear curve fit to the experimental measurements a coefficient of determination (R^2) of 0.9941 is observed designating small linear discrepancy. Due to the degradation of the bonding layer simulated by the insertion

of Teflon, the PZT transducer is enabled to move more freely with less constraint and therefore damping decreases (Nader, Silva, & Adamowski, 2004).

Metrics based on capacitance and the resonance frequency of the PZT are investigated in (Park et al., 2006) and (Mulligan et al., 2012). The capacitance metric performs well in detecting complete transducer debonding but performs poorly in measuring gradual adhesive degradation. This is largely due to resonance peaks that disrupt a linear tendency for the capacitance to increase with debonding. The resonance frequency metric is robust to such peaks and shows a linear tendency to decrease with bonding layer degradation. The sensitivity of the metric is shown in (Mulligan et al., 2012) to be quite low with a range of only 10 %. The modal damping metric ia a combination of the capacitance and resonance frequency metrics and is robust to resonance peaks while providing a range of 100 %.

5. Effects of degradation on actuation and sensing of guided waves

5.1. Experimental setup

In order to relate bonding degradation to the actuation and sensing performance of SHM systems that use PZT transducers, the influence of adhesive layer degradation in a Pitch-Catch configuration is proposed in this section.

For the experimental setup, two transducers are separated by a distance of 20 cm, and fixed to a carbon fiber plate using cyanoacrylate. One transducer is used as a reference, while the other one is used for evaluation of both a degraded actuator and sensor. The Pitch-Catch configuration is surrounded by an absorbing perimeter to attenuate edge reflections. As in section 4.2, Teflon is used to control the amount of adhesive coverage under the PZT transducer as a degradation technique. Between each data acquisition trial, the degraded transducer is removed, the surface is cleaned, and a new transducer is bonded to the plate surface in the same location using a different Teflon mask.

The broadband generation of guided waves through sub-band decomposition technique presented in (Quaegebeur et al., 2012) is used to estimate the transfer functions for amplitude and phase versus frequency below 1 MHz. For a given adhesive coverage degradation, the reference transducer first generates the broadband signals and the degraded transducer is used as a sensor response to estimate the effect of degradation on sensing. Then the degraded transducer is used as an actuator and the reference transducer as a sensor. To determine the effect of degradation on actuation, the amplitude and phase are then frequency averaged for both actuation and sensing for three frequency ranges: below ($<$ 250 kHz), around (250 kHz - 700 kHz), and above ($>$ 700 kHz) mechanical resonance. The adhesive coverage area is known from the Teflon mask areas. The error bars are calculated from the standard deviation of the magnitude of the FFT over each frequency range. The sample size for each standard deviation is approximately 1400 frequency points. The amplitude and phase are presented in Fig. 4 for sensing and in Fig. 5 for actuation.

5.2. Effect of sensor degradation

The amplitude change for a PZT used as a sensor versus adhesive coverage degradation below mechanical resonance is presented in Fig. 4 (a). With degradation, an overall consistent tendency for the amplitude to decrease or increase is not observed. Initially, the amplitude increases 25 % from the perfectly bonded case after 50 % adhesive coverage degradation. Following this, the amplitude decreases 60 % between 50 % - 75 % adhesive degradation. It is also important to note that the error bar at 50 % degradation is 60 % larger than for the other degradation trials. Increasing error bars with adhesive coverage degradation was observed in (Mulligan et al., 2012) with increasing bonding layer degradation largely due to shifting resonance peaks into lower frequency ranges from around and above resonance. These shifting resonance peaks can provide false indications that the amplitude for a specific frequency increases with degradation because the change in amplitude in the figure is determined as an average over the entire frequency range. Smaller frequency range selections can avoid such ambiguities.

The amplitude change versus adhesive coverage degradation around resonance is presented in Fig. 4 (b). In this case, the amplitude decreases with adhesive degradation over a range of 80 %. Again a large error bar is observed at 50 % degradation. The error bar is however 80 % smaller than that of the 50 % degradation trial in low frequency.

The amplitude change versus adhesive coverage degradation above resonance is presented in Fig. 4 (c). As in the around resonance range, the amplitude decreases over a range of 70 %. The error bar in the 25 % degradation trial is now 5 % larger than that at 50 % degradation. This further suggests that resonance peaks are shifting out of high frequency into the other frequency ranges.

The phase change versus adhesive coverage degradation below, around, and above resonance is presented in Fig. 4 (d), (e), and (f). In Fig. 4 (d), the phase of the sensor signal below resonance is presented. With degradation, the phase increases slightly (5^o) from the perfectly bonded case. In Fig. 4 (e), the phase of the sensor signal around resonance is presented. The results show that the phase does not change significantly. For frequencies above resonance shown in Fig. 4 (f), the phase increases slightly (3^o) with degradation.

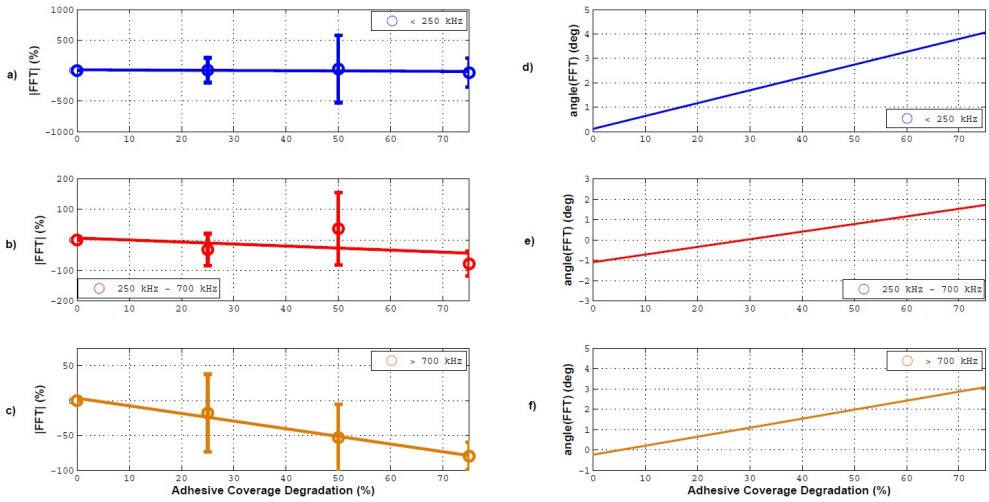

Figure 4. Changes in the amplitude (a,b,c) and phase (d,e,f) of sensor signals with adhesive coverage degradation for three frequency ranges ($<$ 250 kHz: a,d; 250 kHz 700 kHz: b,e; $>$ 700 kHz: c,f).

5.3. Effect of actuator degradation

The amplitude change versus adhesive coverage degradation for a PZT used as an actuator is presented in Fig. 5. In each case, for amplitude (Fig. 5 (a), (b), and (c)), the actuator mimics the same tendencies as the sensor with bonding layer degradation over the same frequency ranges. The amount of amplitude change is in the same range as in the sensor case for all frequency ranges. For the phase, presented in Fig. 5 (d), (e), and (f), each range shows an overall increase with bonding layer degradation. The low and high frequency range increases are identical to those of the sensor case. Around resonance, an increase of 3° is observed. It has been found in literature that bonding layer degradation affects generated signal phase in low frequency which could lead to false indication on structural conditions but the effect has not been studied in ranges higher than resonance (Overly, Park, & Farinholt, 2009).

5.4. Signal correction factor (SCF) for Pitch-Catch measurements

Using the amount of degradation obtained through the modal damping metric and curves that describe changes in amplitude and phase from the perfectly bonded state, a Signal Correction Factor (SCF) is proposed and assessed in the following. The SCF removes biasing in SHM gathered signals from bonding degradation to potentially improve structural damage and RUL estimates (Mulligan, Masson, Létourneau, & Quaegebeur, 2011).

Variations in a signal measured by a transducer within a SHM system are caused by degradation of the host structure $\Delta s^{\text{damaged}}(t)$ and degradation of the transducer bonding layer $\Delta s^{\text{degraded}}(t)$. The measured signal $s'(t)$ can be viewed as the sum of the two components caused by damage on top of a pristine signal $s(t)$ shown in Eq. (2).

$$s'(t) = s(t) + \Delta s^{\text{degraded}}(t) + \Delta s^{\text{damage}}(t) \tag{2}$$

The SCF is derived from the modal damping metric which assesses the level of bonding layer degradation. The change in amplitude and phase for a given degradation and frequency range of the generated signal which are measured empirically, are then used to adjust the captured signal to compensate for the bonding layer degradation measured by the modal damping metric. Next, the changes in amplitude and phase are used as inputs to a formulation for removing the PZT degradation effect to reveal captured signal changes due only to structural damage which is shown in Eq. (3), where the Fast Fourier Transform (FFT) of the measured signal $s'(t)$ is multiplied by an amplitude constant k and a phase shift $e^{j\phi}$. Taking the inverse (IFFT) of the transformed signal leaves the pristine signal changed by structural damage $\Delta s^{\text{damaged}}(t)$. The SCF is therefore defined as SCF = $ke^{j\phi}$.

$$s(t) + \Delta s^{\text{damage}}(t) = IFFT[ke^{j\phi} FFT(s'(t))] \tag{3}$$

The SCF works on the principle that the changes to measured signals due to bonding layer degradation are measurable. Once the amplitude and phase curves with bonding layer degradation are developed either numerically or experimentally for a given material, the modal damping metric is used to assess the level of degradation. The level of degradation is the abscissa on the amplitude and phase curves and with the appropriate adjustment constants, the SCF can be used.

In order to assess the SCF for an extended frequency do-

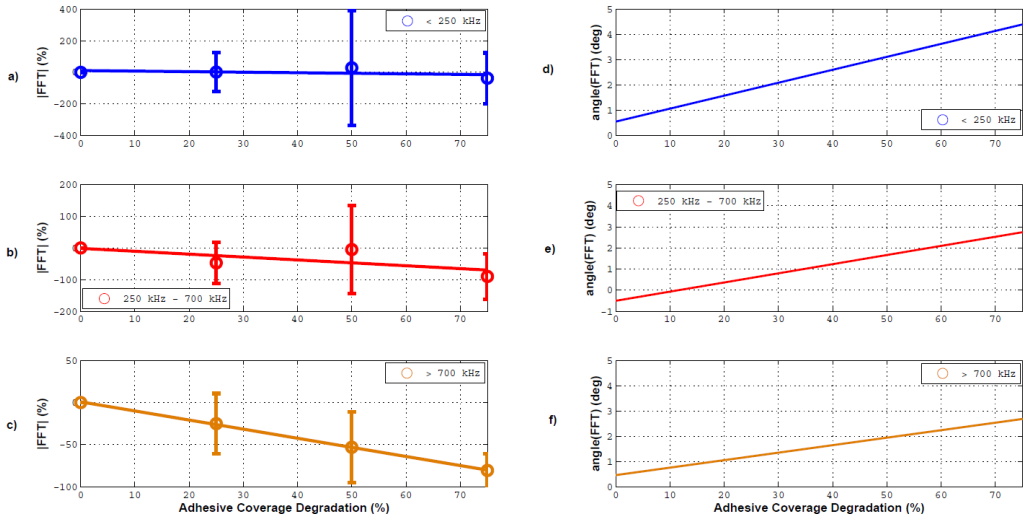

Figure 5. Changes in the amplitude (a,b,c) and phase (d,e,f) of actuator signals with adhesive coverage degradation for three frequency ranges ($<$ 250 kHz: a,d; 250 kHz 700 kHz: b,e; $>$ 700 kHz: c,f).

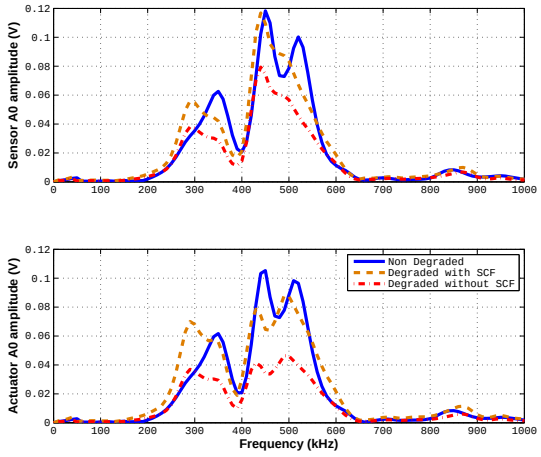

Figure 6. Degraded, non-degraded, and adjusted A_0 modes using the SCF for the sensor and actuator.

main and provide a practical example of feature generation for prognostic model development, the effect of the SCF applied to the A_0 modes is presented in Fig. 6 for a degraded sensor and actuator with 25 % bonding layer coverage degradation. The amplitude of the mode A_0 is extracted separately from the dispersion curves constructed from the signals using sub-band reconstruction (Quaegebeur et al., 2012) over the frequency range below 1 MHz.

In the sensor case, the SCF performs well in adjusting the amplitude of the A_0 mode over the entire frequency range. Around resonance, there is a frequency shift of 10 kHz between the non-degraded and degraded signals that is not accounted for in the SCF. There is also attenuation and deformation of the resonance peaks. These alterations were not observed in (Mulligan et al., 2012). The main difference in the experimental method in this study compared to (Mulligan et al., 2012) is the use of Teflon in the degradation process. Teflon could add damping to the signals received by the PZT and also alter its resonance frequency.

In the actuator case, the SCF performs well in adjusting the amplitude of the A_0 mode over the entire frequency range as in the sensor case. The frequency shift is also observed between the non-degraded and degraded signals although it is a slightly larger shift of 20 kHz compared to the sensor case. Further investigation is required in which the Teflon is removed after the adhesive cures under the PZT. Good performance of the SCF in low frequency is critical in damage imaging (EUSR (Giurgiutiu & Bao, 2004) and Excitelet (Quaegebeur et al., 2012)) and feature generation algorithms as they strongly depend on estimating the Time of Flight (ToF) and amplitude of the A_0 wave packet.

6. Conclusions and Discussions

This paper presented an approach for the correction of data gathered for damage prognosis (DP) in composite structures. To do this, numerical and experimental investigations of the modal damping metric to assess and compensate the degradation of the adhesive layer of surface-bonded PZT transducers for SHM applications is presented. Modal damping curves suggest that the amount of bonding layer degradation is measurable. Bonding layer degradation leads to a reduction in the actuation and sensing amplitude and at higher frequencies, a delay in the time signal is observed. With this information, a Signal Correction Factor (SCF) is used to adjust signals generated or sensed from PZT transducers with a degraded bond-

ing layer. A practical example was demonstrated for the A_0 sensor and actuator signal amplitudes which can be useful in feature generation for prognostics model development.

ACKNOWLEDGMENT

This study has been conducted with the financial support from the Natural Sciences and Engineering Research Council of Canada (NSERC) and the National Research Council of Canada (NRC).

REFERENCES

Ahmad, S., & Gupta, N. K. (2010). Probabilistic analysis of composite panels under low velocity impact. In *Proceedings of the IMPLAST conference.*

ASTM. (2007). *Standard test method for measuring the damage resistance of a fibre–reinforced polymer matrix composite to a drop–weight impact event* (Tech. Rep. Nos. D7136/D7136M–07). American Society for Testing and Materials.

Byington, C. S., Roemer, M. J., & Gallie, T. (2002). Prognostic enhancements to diagnostic systems for improved condition-based maintenance. In *Aerospace conference proceedings.*

Choi, H. (1990). *Damage in graphite/epoxy laminated composites due to low-velocity impact*. Unpublished doctoral dissertation, Stanford University.

Coppe, A., Pais, M. J., Kim, N.-H., & Haftka, R. T. (2010). Identification of equivalent damage growth parameters for general crack geometry. In *Annual conference on prognostics and health management.*

Dupont. (2012). *Teflon PTFE fluoropolymer resin: Properties handbook* (Tech. Rep.). Author.

Farrar, C. R., & Lieven, N. A. J. (2007). Damage prognosis: The future of structural health monitoring. *Phil. Trans. R. Soc. A*, *365*, 623–632.

Galliot, C., Rousseau, J., & Verchery, G. (2012). Drop weight tensile impact testing of adhesively bonded carbon/epoxy laminate joints. *International Journal of Adhesion and Adhesives*, *35*, 68–75.

Giurgiutiu, V., & Bao, J. J. (2004). Embedded-ultrasonics structural radar for in situ structural health monitoring of thin-wall structures. *Structural Health Monitoring*, *3*(2), 121–140.

Iarve, E. V., Gurvich, M. R., Mollenhauer, D. H., Rose, C. A., & Dávila, C. G. (2011). Mesh–independent matrix cracking and delamination modeling in laminated composites. *Int. J. Numer. Meth. Engng*, *88*, 749–773.

Islam, R. A., & Chan, Y. C. (2004). Effect of drop impact energy on contact resistance of anisotropic conductive adhesive film joints. *J. Mater. Res.*, *19*(6), 1662–1668.

Kapoor, H., Boller, C., Giljohann, S., & Braun, C. (2010). Strategies for structural health monitoring implementation potential assessment in aircraft operational life extension considerations. In *Proceedings of the 2nd international symposium on NDT in aerospace.*

Kessler, S. S., & Pramila, R. (2007). Pattern recognition for damage characterization in composite materials. In *Proceedings of the aiaa sdm conference.*

Kim, J., Grisso, B. L., Kim, J. K., Ha, D. S., & Inman, D. J. (2008). Electrical modeling of piezoelectric ceramics for analysis and evaluation of sensory systems. In *IEEE sensors applications symposium.*

Lanzara, G., Yoon, Y., Kim, Y., & Chang, F.-K. (2009). Influence of interface degradation on the performance of piezoelectric actuators. *Journal of Intelligent Material Systems and Structures*, *20*(14), 1699–1710.

Lotters, J. C., Olthuis, W., Veltink, P. H., & Bergveld, P. (1997). The mechanical properties of the rubber elastic polymer polydimethylsiloxane for sensor applications. *J. Micromech. Microeng.*, *7*, 145–147.

Mickens, T., Schulz, M., Sundaresan, M., & Ghoshal, A. (2003). Structural health monitoring of an aircraft joint. *Mechanical Systems and Signal Processing*, *17*(2), 285–303.

Mueller, I., Larrosa, C., Roy, S., Mittal, A., Kuldeep, L., & Chang, F.-K. (2009). An integrated health management and prognostic technology for composite airframe structures. In *Annual conference on prognostics and health management.*

Mulligan, K. R., Masson, P., Létourneau, S., & Quaegebeur, N. (2011). An approach to compensate for the degradation of the monitoring system in damage detection. In *Proceedings of the Canadian Institute for NDE.*

Mulligan, K. R., Quaegebeur, N., Ostiguy, P.-C., Masson, P., & Létourneau, S. (2012). Comparison of metrics to monitor and compensate for piezoceramic degradation in structural health monitoring. *Structural Health Monitoring*.

Nader, G., Silva, E. C. N., & Adamowski, J. C. (2004). Effective damping value of piezoelectric transducer experimental techniques and numerical analysis. In *Abcm symposium series in mechatronics.*

Nguyen, M. Q., Jacombs, S. S., Thomson, R. S., Hachenberg, D., & Scott, M. L. (2005). Simulation of impact on sandwich structures. *Composite Structures*, *67*, 217–227.

Overly, T. G., Park, K., & Farinholt, M. (2009). Piezoelectric active-sensor diagnostics and validation using instantaneous baseline data. *IEEE Sensors Journal*, *9*(11), 1414–11421.

Park, G., Farrar, C. R., Lanza di Scalea, F., & Coccia, S. (2006). Performance assessment and validation of piezoelectric active-sensors in structural health monitoring. *Smart Materials and Structures*, *15*(6), 1673–1683.

Quaegebeur, N., Masson, P., Langlois-Demers, D., & Micheau, P. (2010). Dispersion–based imaging for structural health monitoring using sparse and compact arrays. *Smart Materials and Structures*, *20*(1), 1–12.

Quaegebeur, N., Masson, P., Micheau, P., & Mrad, N. (2012). Broadband generation of ultrasonic guided waves using sub-band decomposition. *IEEE Transactions on Ultrasonics, Ferroelectrics, and Frequency Control*.

Skaja, A., Fernando, D., & Croll, S. (2006). Mechanical property changes and degradation during accelerated weathering of polyester-urethane coatings. *Journal of Coatings Technology and Research*, *3*(1), 41–51.

Sugaya, T., Obuchi, T., & Chiaki, S. (2011). Influences of loading rates on stress-strain relations of cured bulks of brittle and ductile adhesives. *Journal of Solid Mechanics and Materials Engineering*, *5*(12), 921–928.